Christian Stenner, Lee J. Florea, Andreas Pflitsch, Eduardo Cartaya, David A. Riggs. Morphodynamics of glaciovolcanic caves—Mount Rainier, Washington, USA. *Journal of Cave and Karst Studies*, v. 85, nos. 3/4, p. 65-85. DOI:10.4311/2021EX0131

MORPHODYNAMICS OF GLACIOVOLCANIC CAVES – MOUNT RAINIER, WASHINGTON, USA

Christian Stenner[1,C], Lee J. Florea[2], Andreas Pflitsch[3], Eduardo Cartaya[4], and David A. Riggs[4]

Abstract

The twin summit craters of Mount Rainier, Washington, USA host the largest known glaciovolcanic caves in the world and at 4382 m, the highest elevation caves in the USA. The caves are formed in ice at the glacier-rock interface by volcanogenic gases and atmospheric advection. However, the way in which discrete caves are formed and evolve remains poorly understood. Surveys of the cave systems in 1970−1973 and 1997−1998 in both the West and East Craters documented cave passage morphology. Field expeditions from 2014−2017 comprehensively surveyed the Rainier summit caves and undertook thermal imaging and temperature monitoring. Significant changes had occurred. In the East Crater, documented cave length has nearly doubled since 1973 to 3593 m of passage spanning 144 m of depth, revealing a new subglacial lake, and now nearly circumnavigating the East Crater. Of the reported increase in length, some 600 m of the mapped passage is possibly newly formed. Across 47 years of observation, certain sections of the cave appear to be preserved in form and position through time, while others are more actively being lost or forming. Conserved passages are generally sub-horizontal, passages following the curvilinear crater contours, show low temperature variability, and are dependent on perennial fumarolic activity or distributed heat flux emanating from warm bedrock and sediment floors. Transient passages are smaller diameter dendritic passages following the slope of the ice-rock interface towards entrance zones and normal to the circum-crater passage. They also show higher variability in temperature and airflow and are subject to seasonal weather and mechanical collapse, which may contribute to transience. Additional research is required to confirm the mechanisms maintaining conserved passages and formation of transient passages.

INTRODUCTION

Explorable cavities (caves) within glacier ice arise when processes of enlargement locally exceed those leading to closure over a sustained distance. Latent heat in the form of liquid water or water vapor and sensible heat (warm water or air) are the predominant drivers of enlargement. Persistent glacier caves are typically associated with meltwater streams in thin, uncrevassed ice. Studies of glacier caves allow direct observations from a subglacial viewpoint which can calibrate models of rates of glacial melt or movement, bedrock weathering and transport, and glacial outburst floods (Benn et al., 2009).

Volcanoes present a distinct environment where high altitude (or latitude) can permit glaciers, while geothermal heat can cause melting by conduction, fumarole emission, or water flow. A subset of caves formed where glacial ice melts from underlying volcanism, glaciovolcanic caves are rare environments. Curtis and Kyle (2017) reported that of 1443 known subaerial Holocene volcanic centers, 20.3 % (291) are glaciated or have permanent snowfields, while Edwards et al., (2020) identified 245 volcanic centers with potential for impacts from ice. Despite this glaciovolcanism potential, locations with glaciovolcanic caves are not well known at these thermal centers. A review by Sobolewski, et al. (2022a) found limited examples in published literature. Summarized, published studies include sites in Antarctica (Giggenbach, 1976) and both the summit (Kiver and Mumma, 1971; Kiver and Steele, 1975) and Paradise Ice Field (Anderson et al., 1994) of Mount Rainier in Washington, USA (Halliday, 2007). Recent investigations have included discoveries at Mount St. Helens in Washington (Sobolewski, et al., 2022b; Anderson et al., 1998), additions to previous work at Mount Erebus in Antarctica (Curtis, 2010), the role of hydrothermal springs to the cave development at Mount Hood in Oregon (Pflitsch et al., 2017), and exploration on Mount Melbourne and Mount Rittman in Antarctica (Gambino et al., 2021). Curtis (2016) discussed global relevance of glaciovolcanic caves associated directly with fumaroles, derived from examples at Mount Erebus. A comparison of the cave systems compiled from published literature (Table 1) demonstrates the extent and location of the most prominent of the known examples.

The origin and shape of glaciovolcanic caves are intriguing; they originate from and are shaped by the balance between ice accumulation and ablation guided by variations in climate and volcanic heat flux. They are ephemeral landforms. At Mount Rainier, the Paradise Ice Caves disappeared when the ice field melted away from an area of thermal springs (Anderson et al., 1994). At Mount Hood, the Snow Dragon Cave System also largely disappeared as the Sandy Glacier retreated upslope of thermal springs (Pflitsch et al., 2017). In contrast, Crater Glacier and its associated caves

[1] Alberta Speleological Society, Calgary, Alberta, Canada
[2] Washington State Geological Survey, Department of Natural Resources, Olympia, Washington, USA
[3] Institute of Geography, Ruhr-University Bochum, Bochum, Germany
[4] Glacier Cave Explorers, Oregon High Desert Grotto of the National Speleological Society, Redmond, Oregon, USA
[C] Corresponding Author: cstenner@telus.net

Table 1. Comparison of known long and deep glaciovolcanic cave systems.

Cave System	Location	Length (m)	Depth (m)	Reference
East Crater Cave	Mount Rainier, USA	3593	144	Stenner et al., 2022
Mothra Cave	Mount St. Helens, USA	797	72	Unpublished result, 2022[a]
Rodan Cave	Mount St. Helens, USA	775	82	Sobolewski et al., 2022b
MC3 Ice Cave	Mount Melbourne, Antarctica	685	52	Liuzzo, et al., 2018
Warren Cave	Mount Erebus, Antarctica	524	23	Curtis, 2010; 2021[c]
Ghidorah Cave	Mount St. Helens, USA	434	30	Stenner et al., 2020
West Crater Cave	Mount Rainier, USA	308	33	Stenner et al., 2022
Crevasse Cave	Mount St. Helens, USA	276	56	Stenner et al., 2020
Hot Imagination Cave[b]	Mount Hood, USA	273	58	Pflitsch et al., 2017
MC1 Aurora Ice Cave	Mount Melbourne, Antarctica	223	35	Liuzzo, et al., 2018
The Igloo	Mount St. Helens, USA	191	8	Stenner et al., 2020
Kachina Cave	Mount Erebus, Antarctica	146	6	Curtis, 2010; 2021[c]
Snow Dragon System[b]	Mount Hood, USA	2185	292	Pflitsch et al., 2017
Mammoth/Cathedral[c]	Mount Erebus, Antarctica	···	···	Curtis, 2021
Anchor Cave[c]	Mount Erebus, Antarctica	···	···	Curtis, 2021

[a] As of July, 2022 (C. Stenner).
[b] Hot Imagination is a remnant of the Snow Dragon System which is now separately named. The Snow Dragon Cave system length and depth has been significantly reduced by glacial ablation since the reported survey from 2013.
[c] Mammoth/Cathedral system and Anchor Cave at Mount Erebus are likely the longest in the region but are not surveyed. They are reported to be less extensive than the Mount Rainier system (A. Curtis, personal communication, 2021).

in the crater of Mount St. Helens experienced cycles of expansion following the 1980−1986 (Anderson et al., 1998) and 2004−2008 lava dome emplacements (Stenner et al., 2020; Sobolewski et al., 2023). At Crater glacier, persistent low temperature fumaroles combined with glacial expansion contribute to ongoing cave development (Sobolewski et al., 2022b).

Our understanding of glaciovolcanic caves pales in comparison to caves in carbonate rocks (Ford and Williams, 2007), lava tubes (Sauro, et al., 2022; Holler, 2019 p. 836−849), or englacial conduits (Gulley and Fountain, 2019, p. 468−473). Rather, most studies are descriptive or taxonomic and do not focus on process. They represent iterative snapshots of a rapidly evolving environment in the cryosphere, with the six-year-long study on a single glaciovolcanic cave chamber of Mount Erebus (Curtis, 2016) representing the benchmark longitudinal study.

Glaciovolcanic cave morphodynamics suggested as an indicator for volcanic activity (Curtis, 2016; Zimbelman et al., 2000) remains an unproven hypothesis. Six years of observation in Warren Cave at Mount Erebus could not link dynamic morphology to changes in volcanic activity (Curtis, 2016). Rather, Curtis (2016) suggested that new glaciovolcanic cave development may indicate subnivean volcanic unrest. A recent example of glaciovolcanic cave genesis in the glacier at Mount Meager, Canada have raised concerns about renewed volcanic hazards (Roberti, 2018; Unnsteinsson, 2022).

Studies thus far demonstrate persistent warm gas emissions from fumaroles and spatial discrete air movement by convection or advection distribute heat from point sources along cave passages (Curtis and Kyle, 2011). Analytical and numerical modeling of glaciovolcanic void formation fitted functions of glacier thickness, heat flux, vertical ice velocity, and bed slope to the height of a void (Unnsteinsson, 2022). Suppression or closure of voids is predominantly due to ice flow (creep) (Unnsteinsson, 2022) or mechanical collapse (Sobolewski, et al., 2022b). However, results from glaciovolcanic cave studies have yet to understand and classify cave geometry and potential variability.

Table 1 reveals the disparity between the Mount Rainier cave system and others; it offers an extensive setting to observe glaciovolcanic processes among the limited known examples. Here, mapping and monitoring of glaciovolcanic caves on Mount Rainier are used to see if configuration changes at a decadal time scale.

PHYSICAL SETTING

Mount Rainier formed through successive eruptions over the past 840 ka; the current East and West Craters are nested in the remnants of an older and higher edifice that collapsed approximately 540 ka ago. Eruptions are documented throughout the Holocene along with recent activity in the 19th Century. Evidence of magmatic eruption from 1 ka BP exists while observers reported the most recent eruption in December 1894; this may have impacted summit ice though confirmation is lacking (Sisson and Vallance, 2009). A prior verifiable eruption impacting summit ice occurred between 1820 and 1840 along with observations of a subaerial crater lake (Frank, 1995). Past impacts to the surround-

ings include extensive lahars of up to 3 × 10^9 m^3 (Crandell, 1971; Scott et al., 1995) with the Osceola mudflow being the largest one in the volcano´s recent history (Vallance and Scott, 1997). An extensive glacial system is supported on the volcano flanks, however glacial ice volume has reduced 25 % overall since 1913, while 14 % volume loss occurred between 1970 and 2008, as mean annual temperatures increased and snowfall decreased (Hoffman et al., 2014, Nylen, 2004; Sisson et al., 2011).

With increasing glacial melt observed at Rainier comes the potential for enhanced hydrothermal activity as active snow and ice melt at the summit craters and alteration product deposition (Frank, 1995; Korosec, 1989) lead to increased bedrock alteration, weakening slope stability, leading to mass wasting (Finn et al., 2001). The culminating effects of reduced glacial mass and edifice stability may increase the probability of eruption (Capra, 2008; Tuffen, 2010). More than 100 fumaroles, driven by hydrothermal cycling of glacial melt, presently exist under the summit ice plugs and flanking glaciers (Frank, 1995). As a consequence, Mount Rainier has a need for increased hydrothermal and fumarole monitoring (National Research Council, 1994). Potential impact to nearby populations due to lahars, amongst other hazards, resulted in Mount Rainier's designation as a Decade Volcano in 1987 by the International Association of Volcanology and Chemistry of the Earth's Interior and a high risk site in the United States Geological Survey (USGS) National Volcanic Early Warning System (Ewert et al., 2018).

Glaciovolcanic Caves – Mount Rainier

The twin summit craters of Mount Rainier house the East Crater and West Crater Caves, the East Crater Cave being the longest and deepest known (Table 1; Fig. 1). These were first identified during the 1870 summit climb by Van Trump and Stevens (Stevens, 1876). Whittaker (1957) described his entry into the caves in 1954. Whittaker and Nelson

Figure 1. Base map of the Pacific Northwest, United States of America showing location of Mount Rainier and other Cascade volcanoes. Inset image of the surveyed extent of the East and West Crater cave system passages at the summit of Mount Rainier, marked in red and blue and overlaid on GIS satellite imagery (ESRI and Google Earth).

returned in 1970 and made a traverse to a second exit (Wilkins, 1970) and produced the first known grade 1 sketch (Fig. 2a). Project Crater (Kiver and Mumma, 1971; Lokey et al., 1972; Lokey, 1973) conducted a geophysical study and mapping effort of the East and West craters from 1970−1973 and produced the first detailed planform cave maps (Figs.

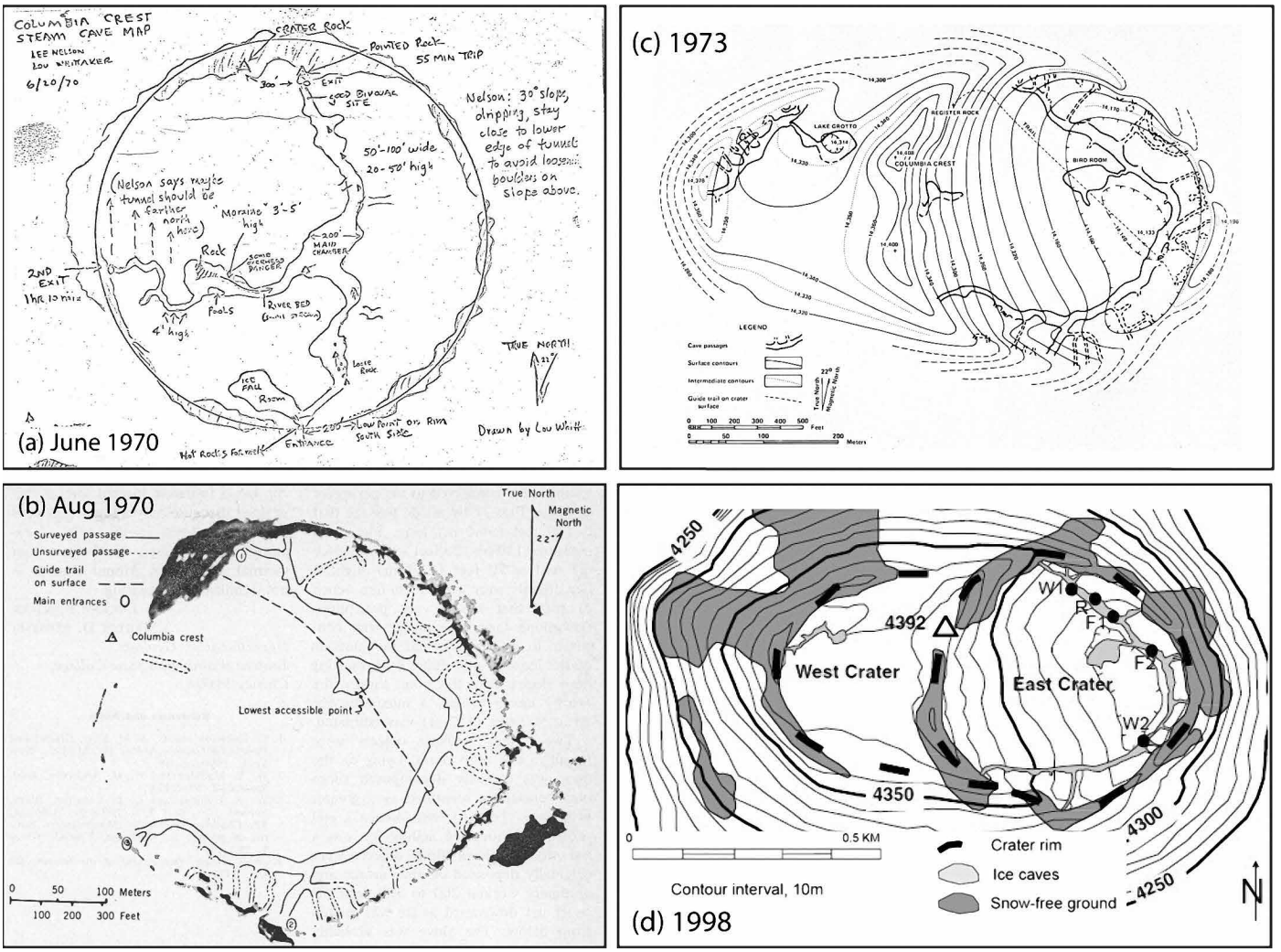

Figure 2. Historical planform surveys used for comparative analysis. (a) Grade 1 survey of East Crater Cave by Nelson and Whittaker (1970). (b) Survey reported in Kiver and Mumma (1971). (c) Surveys of East Crater Cave and West Crater Caves from Kiver and Steele (1975), and (d) Surveys of East Crater Cave and West Crater Caves from Zimbelman, et al., (2000).

2b and c) comprising 1800 m in the East Crater and 305 m of passages in the West Crater, including Lake Muriel below the West Crater ice (Kiver and Steele, 1975). These first tripod mounted compass surveys provide a baseline for comparisons. In 1997, a team of USGS and National Park Service scientists conducted studies (Le Guern et al., 2000; Zimbelman et al., 2000), and produced a fourth map iteration that included 700−1500 m of passage in the East Crater Cave and 155 m of passage in the West Crater Cave, (Fig. 2d).

We conducted sequential studies in the craters of Mount Rainier from 2015−2017. In August 2015, an expedition of 16 stayed on the summit for 9 days to study and map the East and West Crater Caves. In East Crater, 3170 m of passage were surveyed spanning 112 m of depth. In the West Crater, high CO_2 concentrations limited exploration to 137 m of surveyed passage. With over 50 personnel transporting gear and conducting studies on climatology, geochemistry, hydrology, microbiology, and glaciology, the 2015 expedition was the largest known operational event to occur in the history of Mount Rainier National Park (Cartaya, 2016). A smaller, five-day summit expedition in July−August 2016 placed and downloaded data from dataloggers, measured passage volume, collected thermal images, and monitored gas readings.

In July−August 2017, an expedition of 14 returned to the summit to support cave survey and research in climatology, geochemistry, as well as tests by NASA Jet Propulsion Laboratory of prototype robotic technologies for ice climbing and core sampling, given the utility of the cave as an ocean world analog. Eighty personnel were involved, carrying

680 kg of equipment to the summit and back over a span of 13 days. A replicate survey in the East Crater Cave included remaining leads, such as the Bird Room, the deepest point. In the West Crater, the cave was fully explored using Self-Contained Breathing Apparatus (SCBA). (Stenner, et al., 2022). A companion paper to this study, Stenner et al. (2022), discussed hazardous atmospheres due to fumarolic degassing in the Mount Rainier system, whereby turbulent and convectively rising gas and vapor plumes from the subglacial fumarole vents circulate within the cave system and cause CO_2 accumulations.

Mount Rainier Cave Morphodynamics and Volcanic Activity

Depictions of geometric changes have been proposed as indicators of volcanism in the Mount Rainier caves but have been anecdotal (e.g., Anon, 1972). Kiver and Steele (1975) noted enlargement of the cave passages over four years and suggested the system may not be in equilibrium, and that changes may be a normal condition. They proposed that changes in summit thermal activity would cause corresponding changes in cave passage location, size, and morphology, accompanied by an increase in micro-seismic activity. Hoblitt et al. (1998) noted a reawakening Mount Rainier would cause increased gas emissions in the caves. Zimbelman, et al., (2000, p. 462) further noted that "Because the caves act as condensers, traps, and calorimeters for magmatic volatiles and heat, their characterization and monitoring may represent powerful potential indicators of changes in the hydrovolcanic system which may not be readily apparent by surface surveys."

More recently Florea et al., (2021), using a year of continuous monitoring data, identified a dynamic equilibrium of the Rainier summit caves responding to seasonal weather patterns and temperature changes. During winter storms, entrances seal and advection diminishes, leading to increased temperatures and subglacial melt until entrances re-open. These observations lead to a hypothesis that changes in passage position and morphology are present in the dynamic equilibrium of the Mount Rainier cave system, but observable only over longer timescales.

In this study, we compare data from a review of literature and historical cave surveys on the Rainier summit to our most recent cave passage and fumarole location survey, passage ablation measurements, and vertical ice movement measurement to quantify passage characteristics and the potential degree and magnitude of change through time. This multi-decadal (47 year) comparison is the first of which we are aware and aims to add to our understanding of the morphodynamics of an understudied subset of speleology. Using available preliminary temperature and thermography data we support the comparison and discussion on mechanisms of observed changes. Our results lead toward a model for the origin and morphology of glaciovolcanic caves applicable to other glacial-mantled volcanic edifices.

METHODS

Survey and Cartography

Tacheometric cave surveying methods used fixed stations to map passage extent, cross-section, datalogger locations, ablation markers, fumaroles, and cave entrances during 2015−2017 fieldwork. In-cave reference stations provided fixed locations for connecting annual surveys. Nine surface stations at entrances were referenced using global navigation satellite systems (GNSS). A transect survey over the glacier surface from the Guide Rocks entrance to the crater rim adjacent to the Misery Crawl entrance connected ice surface elevation to the cave survey. All survey data were collected using calibrated DistoX2 (a custom Leica A3 rangefinder modified to provide distance, azimuth, and inclination) paired with a Windows Mobile Dell Axim X51 Personal Digital Assistant (PDA) using PocketTopo software (e.g., Heeb, 2009; n.d.).

Several challenges inhibited efficiency, and potentially, accuracy in this study. First, survey stations on unstable rocks disappeared between study years, as rocks themselves had fallen down passages or having degraded in the harsh environment, requiring creation of new stations. As mitigation, 1.5 mm × 6 mm aluminum rivets were installed in rocks with a reflective tag at nine stations. Next, visibility in the caves was sometimes obscured by thick steam from fumaroles, limiting DistoX2 measurements for passage cross section and volume. Additionally, volcanic boulders rich in mafic minerals caused magnetic interference and deflected azimuth measurements by up to 15 degrees, requiring offset (floating) stations as mitigation.

After reviewing the raw data, we calculated passage cross section and volume in East Crater Cave using the splay shots radiating from two recoverable reference stations at repeatable azimuths and inclinations in 2016 and again in 2017 (Fig. 3). Of the 195 splay shots at these reference locations, 53 were within a 1.5-degree range of their previous companion measurement and considered suitable for comparison.

Post processing of 2015−2017 survey data used Compass cave survey management software (Fish, 2020). Loop closure and GNSS reference points at entrances (Fig. 4a) helped mitigate any unknown survey errors, including magnetic interference. Using a script and a line-by-line review, splay measurements were converted to left, right, up, down distances normal to the direction of survey so that Compass could generate passage volume. We used Adobe Illustrator for cartography and CaveXO for 3D visualizations and produced a video visualization and 3D shapefile archive.

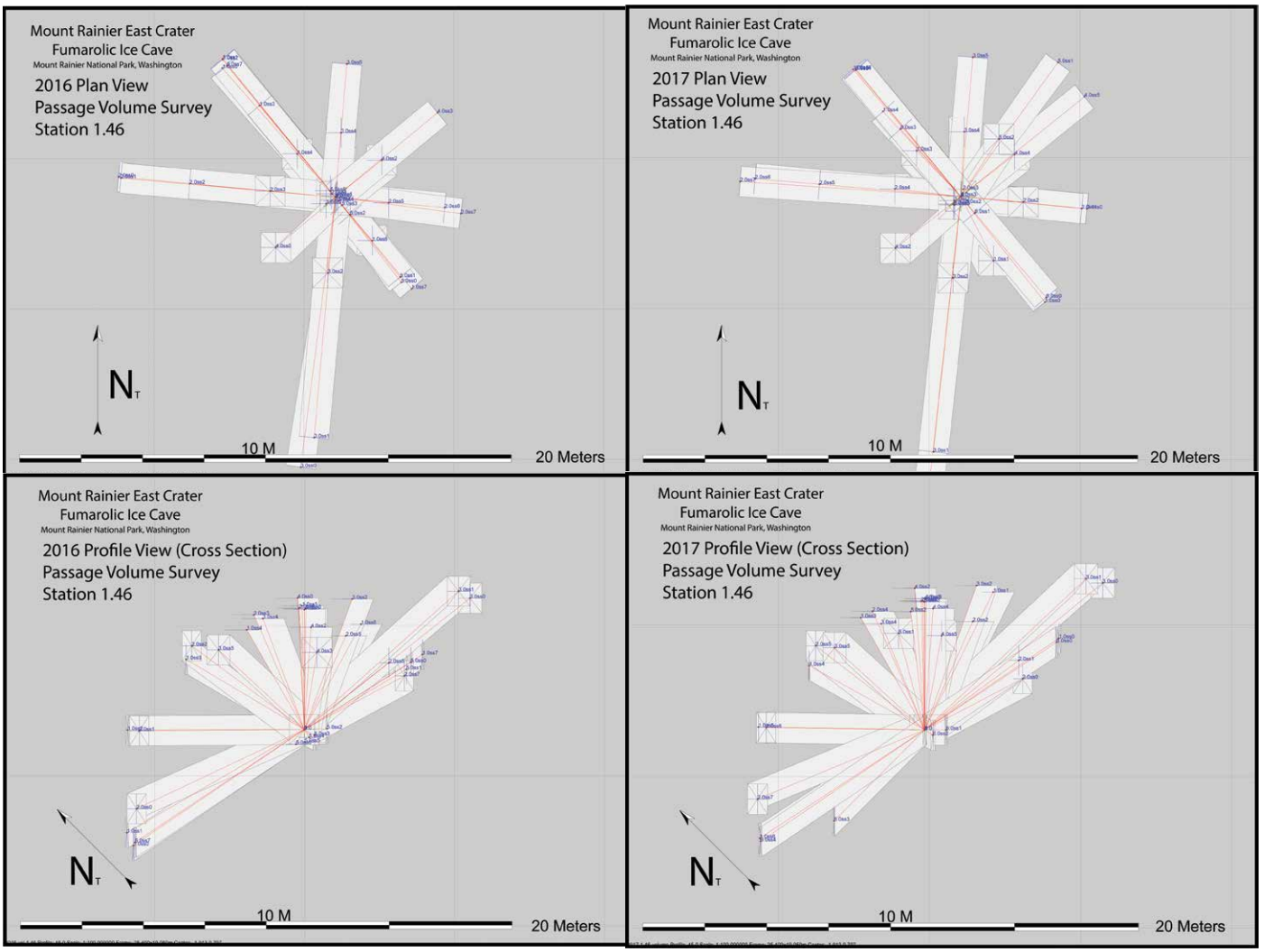

Figure 3. Imagery generated using Compass, representative of survey method used for passage volume surveys in 2016 and 2017 at stations 1.46 and 1.48. The images in plan and profile view, from station 1.46, represent 38 survey shots repeated in 2016 and 2017 with values reported in Table 5.

Surveys are graded UISv2 5-3 BCEF, which allows error ratios of 0.05 m for survey shot length, 1 degree for azimuth and inclinometer measurements, and 2 % overall as per Häuselmann (2012), while GNSS stations are estimated to be accurate within 2−3 m.

Longitudinal comparison was facilitated by a synthesis of reported refereed and historical literature related to the Mount Rainier summit cave system. Literature searches revealed refereed sources and related reports, which were included when observations or data existed regarding the cave system. For historical surveys of the Rainier caves, published planform maps were converted to vector graphics using Adobe Illustrator. Georeferencing and scaling those maps for comparative analysis required aligning crater rim landmarks between those surveys and our own, including the summit (Columbia Crest) and three prominent ridges of the crater rim on the North, West and East side. Stacking the sequential surveys in an overlay made changes easier to qualitatively visualize and communicate. From the overlay comparison, passages were considered potentially consistent if their overlaid positions overlapped, or not consistent if their positions did not. These segments were then isolated in Compass to generate characterization data on each.

Climate and Ablation Monitoring

Methods and equipment used for data collection by Florea et al. (2021) are described therein and supplement original, preliminary data in this manuscript, meant to support a longer-term climate monitoring synthesis. New to this paper are air temperatures measured every 10 minutes at nine locations using Geoprecision M-Log5W-CABLE dataloggers with accuracy: ±0.1 °C at 0 °C (Fig. 4a). Four of the sites were in the circumferential passage: Hobo Point between the passages that lead to the Yeti and Murphy's Law entrances, Main Passage 1 below the Aircrash Entrance, Main Passage 2 be-

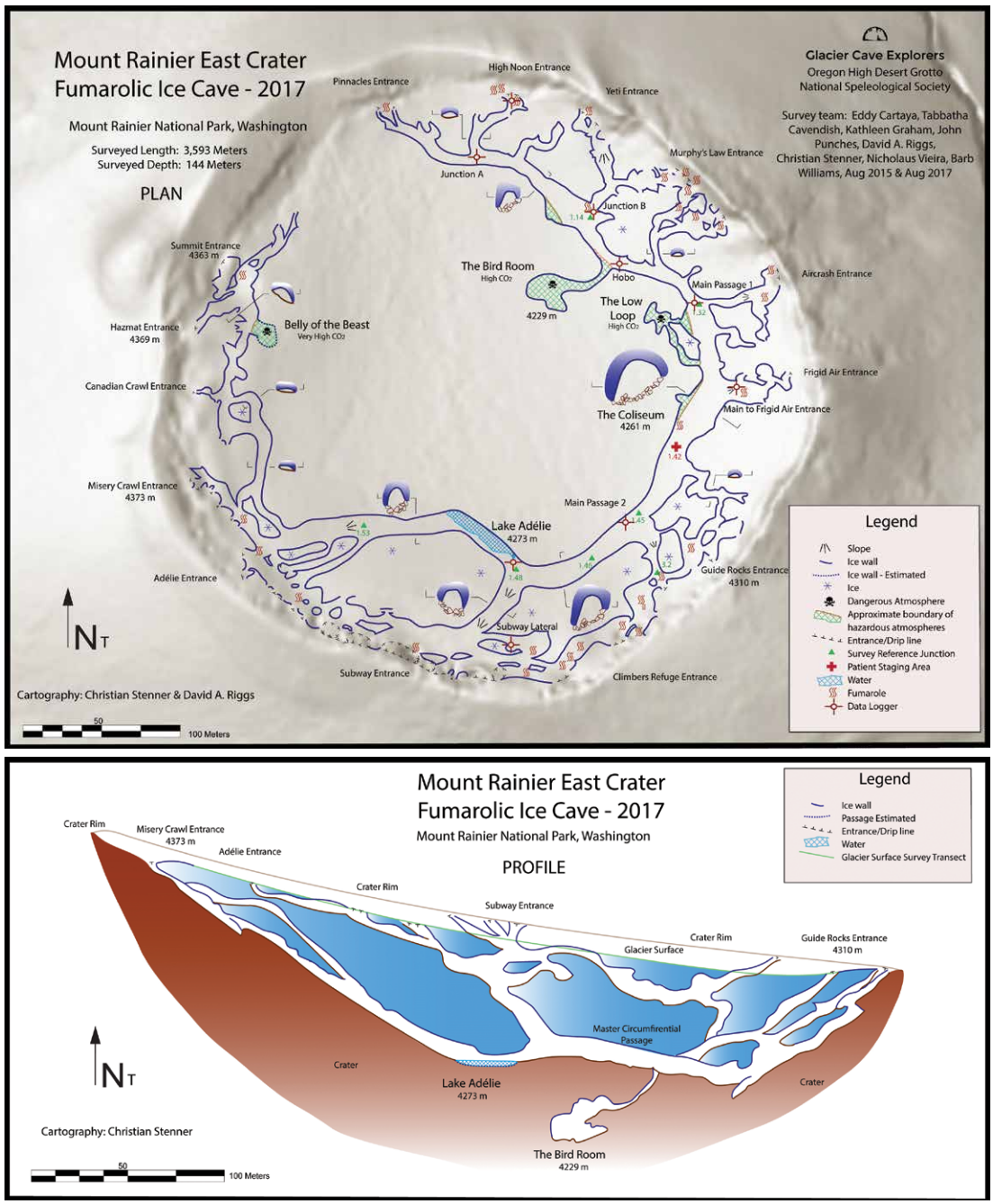

Figure 4. (a) Survey in plan view of the East Crater Cave. Map legend lists key features. Base map is a combination of digital elevation hillshade and satellite imagery (ESRI and Google Earth). Survey indicates locations of data loggers, passage survey reference stations including the locations of passage volume (1.48 and 1.46) and ice ablation studies (1.46). (b) East Crater cave profile looking north, indicating glacier surface transect and key entrances. Foreground passages are shown as viewed looking north. Northernmost entrance passages are omitted for clarity.

low the Guide Rocks Entrance, and near Lake Adélie. Five additional sites were situated near or in the passages leading to entrances: Pinnacles, Yeti, High Noon, Frigid, and Subway. One site recorded data from August 2015 to August 2016 (Subway Entrance,) five from August 2016 to August 2017 (Junction A, Junction B, High Noon, Lake, Frigid Air), and the remaining two from August 2015 to August 2017 (Aircrash, Guide Rocks). Thermographic cameras (VarioCam High Resolution, Jenoptik) recorded ordinal measurements of fumarole locations and cave floor temperatures. In 2015, we imaged the circumferential passage between the Yeti Entrance and Lake Adélie. In 2017, time-series images of a fumarole area near the High Noon Entrance were collected. Three individual fumaroles were instrumented with temperature dataloggers and those data are presented in Florea et al. (2021). Thermographic video is available upon request.

The vertical rate of crater ice ablation was challenging to measure during our expeditions despite various attempts and methods. In our only successful attempt, four plastic markers were installed in the wall of the East Crater Cave at two-meter intervals along with an ice-screw used to aid ice climbing at a maximum height of eight meters (Fig. 4a). All markers and the screw were referenced by survey shots to a nearby fixed station with remeasurement intended to calculate vertical movement and ice residence. All four plastic ablation markers were found on the cave floor the next year; ice squeezing and melt-out caused almost all types of markers to be ejected over time. However, the ice screw was intact in the ice but deformed by pressure against boulders on the cave floor.

RESULTS

Survey Statistics

The 2015−2017 East Crater Cave survey includes 6635 individual survey shots and comprises 3593.3 m of passage that nearly circumnavigates the crater rim and includes 20 separate entrances (Fig. 4a) (Table 2). The highest elevation entrance is at 4373 m and the lowest point is the Bird Room at 4229 m, a vertical range of 144 m (Fig. 4b). Using our ice surface transect, the ice thickness over the circumferential passage floor averaged 47.4 m with a maximum value of 64.6 m (visualized as a thin line across the cave passage in the video of 3D model, Appendix 1). The Bird Room was

Table 2. Survey data from Mount Rainier East and West Crater Cave expeditions, 2015−2017.

Parameter[a]	Units	East Crater	West Crater	Notes[b]
Cave Length	m	3,593.3	307.7	Total length of surveyed segments
Total Surveyed	m	37,303.1	2,487.5	Includes all splay measurements
Cave Depth	m	144.1	33.6	Difference between highest and lowest stations
Cave Volume	m^3	154,018.5	15,477.2	Volume of cave passages based on LRUD data
Average Diameter	m	6.6	7.1	Average passage diameter based on LRUD data
Highest Station	m	4,373.3	4,381.7	···
Lowest Station	m	4,228.5	4,348.1	···

a A 2 % overall error ratio is estimated as per Häuselmann (2012) given the survey methods used.
b Descriptive note regarding the statistical data from Compass derived from Fish (2020).

95 m below the surface transect. Using our single ablation measurement, vertical ice movement was 8.4 m y^{-1} and the residence time was ~7 years for the ice thickness of 57.3 m at the measurement location. Assuming the past estimate of 120 m total ice thickness in the crater (Table 3), and the same rate, the maximum residence time would be ~14 years. The cave includes a circumferential main passage following the strike of the crater with steeply dipping, and perpendicular entrance passages connecting this main passage to the crater rim, visualized in the profile (Fig. 4b), video and data file (Appendix 1).

Table 3. Comparison of Mount Rainier crater caves reported speleometric and morphology data, 1970−2017.

Feature	Cave Dimension per Study Date (m)				Notes
	1970[a]	1973[a, b]	1997[a]	2015−2017[c]	
			East Crater Cave		
East Crater Cave Length	1737	1800	>1500[d]	3593	
East Crater Cave Depth	···	123	···	144	
East Crater number of entrances	~24	~16	12[e]	20	
Main perimeter passage length	915	915	720[e]	999	
Main perimeter passage depth	61	70	···	64.6	
Main passage dimensions	7.6−10.6 × 4.6	15 × 6	15 × -[e]	15 × 6	W × H avg.
Highest point elevation (a.s.l.)	···	4338[e]	···	4373	
Deepest point elevation (a.s.l.)	4228	4215	···	4229	
Deepest point to crater bottom	31.7[e]	~16	···	···	
Deepest point to ice surface	91	~104	···	95	
			East Crater Cave features		
Bird Room dimensions	36.6 × 36.6 × 21.3	54 × 36 × 21	62 × 43 × ···[e]	34 × 30 × 22	L × W × H
Lake Adélie dimensions	···	···	···	50 × 5 × 7	L × W × D
Lake Adélie surface area	···	···	···	~250[f]	
Lake Adélie elevation a.s.l.	···	···	···	4273	

[a] A 2%-5% overall error ratio is estimated as per Häuselmann (2012) given the survey method.
[b] Vertical and horizontal passage position error ratios are ~10 m (Kiver and Steele, 1975).
[c] A 2% overall error ratio is estimated as per Häuselmann (2012) given the survey method.
[d] The 1997 efforts reported a total length of 700 m in the East Crater Cave (Le Guern et al., 2000) whereas Zimbelman (2000) reported more than 1500 m; 700 m is likely a reflection of the length of the main perimeter passage as it is estimated as 720 m long based on the published survey.
[e] Estimated values extrapolated from published survey/data.
[f] Surface area has units of m^2.

In the West Crater Cave, 364 individual survey shots encompass 307.8 m of passage (Table 2). The vertical range spans 33.6 m to the deepest point in the Canary Room. In this paper, we will focus on the East Crater.

Comparative Morphology

The vectorized cave maps from prior expeditions, cartographic plans from our expeditions, and passage volume measurements from 2015−2017 (Table 2) allow comparisons over a 47-year timeframe. As raw survey data were not available from expeditions in the 1970s and 1990s, comparisons were made by extrapolating from statistics and plan-form surveys available in Kiver and Mumma (1971), Kiver and Steele (1975), and Zimbelman et al., (2000) (Fig. 2; Table 3). Profile view surveys and passage cross sections were not published in those studies.

Classification of passage orientations were conducted to aid characterization. Glaciovolcanic passage orientation is constrained by the surface underlying the ice. Where the passage followed sub-horizontal direction, typically towards the center of the crater with downward inclination it was considered dip oriented. Strike-oriented passages were those following the curvilinear contour and not oriented downwards towards the crater center. Limited passage collections were grouped as mixed strike and dip where short sections of maze-like geometries were encountered.

An overlay of all cave surveys (Fig. 5) reveals areas of overlap; the heatmap indicates where passage position remained consistent over 47 years. Areas with three and with four surveys where overlap occurred were color coded and the passages were considered to have positional consistency. As previous surveys included many estimated passages (dashed lines, e.g., Figs. 2b and c) and survey precision could not be resolved they were excluded from these criteria.

To determine characteristics for the observed consistent and inconsistent passages (Fig. 5), the passages were then divided into segments based on their orientation classifications of either dip oriented or oriented along the curvilinear strike. As dip-oriented segments were typically adjoining the master curvilinear passage at their bottom end and crater entrances at the rim at their top end, these provided distinct segments that could be isolated to derive further speleometric data in Compass and align with temperature and fumarole survey data (Table 4).

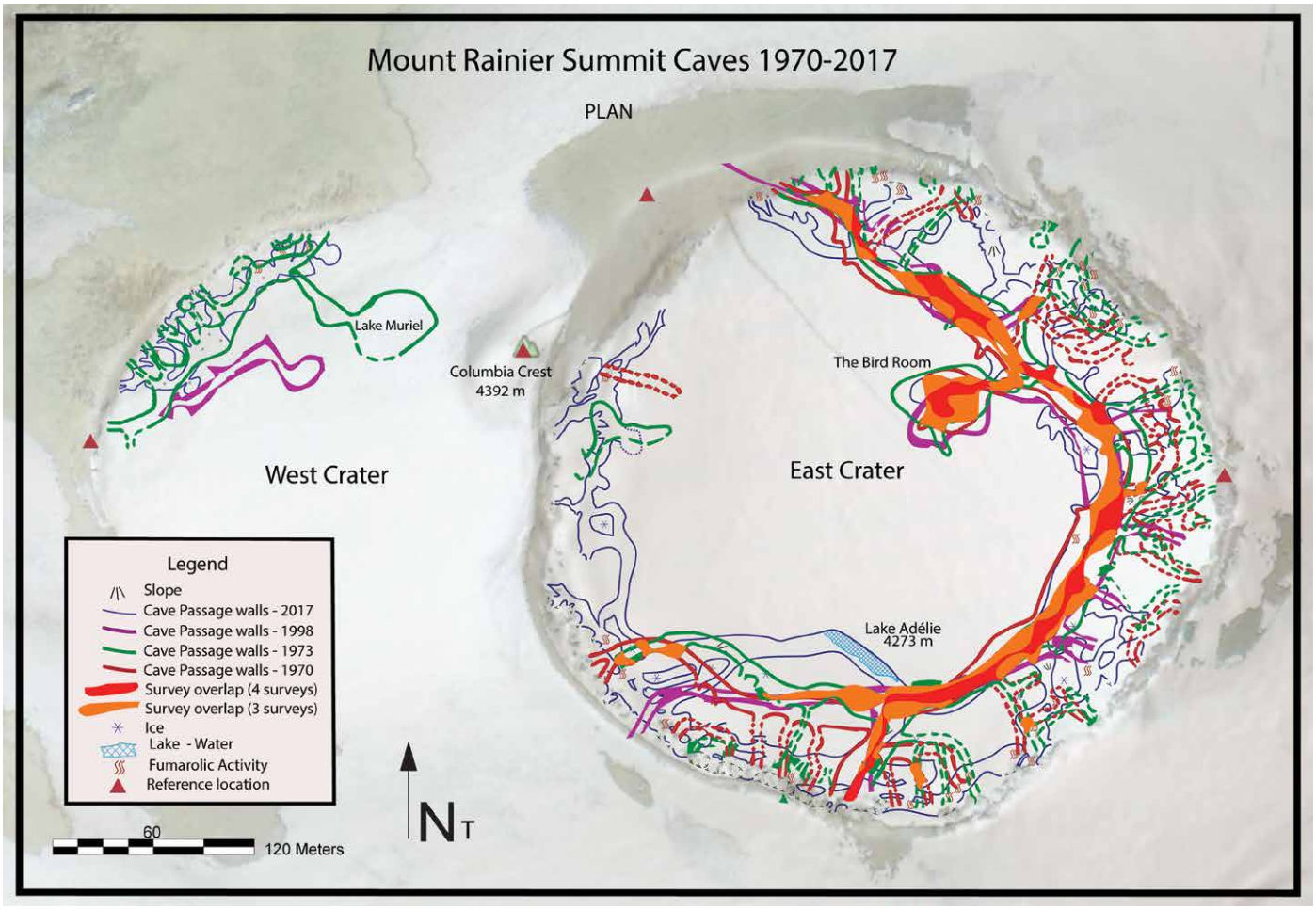

Figure 5. Overlay of corrected and georegistered passage wall planform surveys from 1970−2017. Red-orange heatmap indicates areas where passage overlap occurred between three or four surveys. Four reference locations shown were used to align surveys. Base map is from satellite imagery (Google Earth).

Table 4. Mount Rainier East Crater Cave segments and air temperature data.

Passage Name	Orientation Classification	Planform Consistency	Average Inclination (m)	Average Diameter (m)	Temperature			
					Min (°C)	Max (°C)	Mean (°C)	Variance[a] (C°)
Low Loop	Dip	Unresolved	19.8	2.1	···	···	···	···
Small lead Aircrash South	Dip	Unresolved	31.2	3.0	···	···	···	···
Coliseum to Guide Rocks	Dip	Unresolved	25.3	3.9	···	···	···	···
Small lead Aircrash North	Dip	Unresolved	30.0	3.5	···	···	···	···
Branch South of High Noon	Dip	Unresolved	21.0	1.9	···	···	···	···
Aircrash entrance connection	Dip	Unresolved	30.4	3.0	···	···	···	···
Yeti East (Junction B)	Dip	Unresolved	19.1	3.7	−14.7	9.6	2.8	13.7
High Noon entrance (2017)	Dip	Unresolved	21.2	3.9	−9.6	9.4	2.1	5.6
Yeti lower connection	Dip	Unresolved	30.2	4.8	···	···	···	···
Adélie small tributary	Dip	Unresolved	30.7	0.7	···	···	···	···
Lake Adélie entrance down	Dip	Unresolved	35.5	5.7	···	···	···	···
Subway Entrance down	Dip	Consistent 3−4 surveys	30.3	7.1	···	···	···	···
Bird Room and connection	Dip	Consistent 3−4 surveys	26.5	7.4	···	···	···	···
Adélie to subway upper maze	Mixed	Unresolved	21.0	3.6	···	···	···	···
West Extension	Mixed	Unresolved	19.4	2.3	···	···	···	···
Pinnacles entrance (Junction A)	Mixed	Unresolved	30.1	3.7	−12.4	6.8	1.4	8.2
Columbia Crest area	Mixed	Unresolved	18.7	4.2	···	···	···	···
Climbers Refuge maze	Mixed	Unresolved	25.8	6.0	···	···	···	···
Main borehole to Frigid ent. (2017)	Mixed	Unresolved	28.7	4.9	−9.5	10	0.8	7.8
Yeti upper lateral section	Strike	Unresolved	25.8	3.4	···	···	···	···
Belly of Beast near summit	Strike	Unresolved	24.5	2.3	···	···	···	···
Climbers refuge area	Strike	Unresolved	20.2	6.4	···	···	···	···
Subway lateral area (2016)	Strike	Unresolved	15.4	3.9	−15.5	3.3	0.1	4.6
Aircrash entrance lateral	Strike	Unresolved	25.8	6.0	···	···	···	···
Yeti to Murphy's law entrance	Strike	Unresolved	24.9	3.6	···	···	···	···
Master curvilinear passage	Strike	Consistent 3−4 surveys	14.7	7.8				
Hobo point (2017)	···	···	···	···	−9.5	6.4	1.7	3.8
Main passage 1 (2016)	···	···	···	···	−8.9	8.1	2.1	4.8
Main passage 1 (2017)	···	···	···	···	−8.9	7.7	2.3	4.7
Main passage 2 (2016)	···	···	···	···	−5.7	5.3	1.8	2.5
Main passage 2 (2017)	···	···	···	···	−4.5	5.6	1.9	1.8
Lake Adélie East	···	···	···	···	−6.9	5.4	1.2	1.4

[a] Average of the squared differences from the mean.

From these criteria, most of the master curvilinear passage showed consistency across multiple surveys, from the East side of Lake Adélie (Fig. 6a) until just before the 2017 Pinnacles entrance. The Bird Room (Fig. 6b), along with the passage connecting the East side of Lake Adélie to the Subway entrance also showed consistency across multiple surveys.

The remaining segments changed considerably from earlier planform surveys or could not be resolved to have positional consistency due to expected survey errors or in that previous surveys of those passages were estimates of position and geometry. Our comparison reveals three main areas of change in East Crater Cave. First, a shift in the circumferential passage at the southwest end of East Crater Cave where all historical surveys demonstrate the passage as higher up the crater rim; Lake Adélie is only represented on the most recent survey. Second, 598 m of additional passages were surveyed in 2015−2017 on the west side of East Crater starting from the westernmost limits of all previous

Figure 6. (a) East side of Lake Adélie, East Crater Cave. (b) The Bird Room, East Crater Cave, showing inclination of the floor surface and ablation scalloping difference on cave walls compared to master circumferential passages.

maps and nearly completing the crater circumnavigation, lacking 82 m of intervening distance (Figs. 4a and 5). At least three fumaroles were located in this extension, which had an average passage diameter of 4.7 m. The resulting passage extension wraps around the west side of the East Crater. Third, none of the dendritic passages radiating outward from the master curvilinear passage and entrances along the crater rim remained consistent across the surveys excepting the passage connecting Lake Adélie to the surface (Fig. 5).

Comparative cross section and planform measurements from two survey stations (Figs. 3 and 4a) across 2016−2017 are reported in Appendix 2 and summarized in Table 5. The mean increase in distance from station to the walls was 0.13 m across both locations.

Thermographic Survey

Thermal camera recordings clearly identified individual fumarole vents emitting vapor or gas in fumarole fields on the crater floor (Fig. 7a). Additionally, areas of heated sediment or rock were present. In the circumferential passage between the Yeti Entrance and Lake Adélie, we identified 9 areas of high heat flux each with more than 10 spots above 30 °C and up to 51 °C, and an additional 11 areas with 1−9 spots above 30 °C. These areas of heat flux alternate with zones with no or little fumarole activity to form a ring coincident with the circumferential passage (Fig. 7b). We documented another discontinuous ring of fumaroles above 30 °C near the crater rim (Fig. 4a) that, unlike the lower circumferential passage, no continuous passage connects those fumaroles but they are coincident with many entrances. Thermographic recordings in 2017 near the High Noon Entrance showed temperature variations of up to 15 °C on the crater floor over time spans of a few hours.

Air Temperature

Time-series graphs of the measured air temperature compiled from dataloggers are presented in Figure 8, with summary statistics in Table 4. Further descriptive information on the datalogger locations and influences are offered below.

Main Passage 2, offset from the passage that leads to the Guide Rocks Entrance, was not directly affected by fumaroles and remained mostly free of fog. At Main Passage 1, offset from the passage that leads to the Aircrash Entrance,

Table 5. Mount Rainier East Crater Cave main passage volume measurements, 2016−2017.

Azimuth measured (deg / deg)	Change (m)[a]
Lake East (station 1.48)	
65 / 245	0.28
155 / 335	0.58
290 / 110	−0.61
20 / 200	−0.40
200 / 20	0.13
Mean	−0.01
Change[a]	0.13
Coliseum (station 1.46)	
140 / 320	−0.00
320 / 140	0.21
95 / 275	0.09
5 / 185	0.40
50 / 230	0.72
Mean	0.24
Change[a]	0.13

[a] Mean difference in meters between comparative measurements made in 2016 and repeated in 2017.

numerous fumaroles were observed during fieldwork to cause a prevailing dense fog and airflow was toward the entrance. The Subway Entrance site is approximately five meters below the Subway Entrance in a larger space at the top of the vertical shaft extending to the main passage.

In 2016−2017 additional measurement sites were added (Table 4). Junction A is below the High Noon entrance, as well as the Pinnacles entrance, and is defined by two entrances to the outside as well as the connection to the main curvilinear passage. No fumaroles exist in the vicinity of the datalogger. Junction B is located in a large dome-like hall on a slope directly below the passage to the Yeti and the Murphy's Law entrances, and is thus influenced by two connections to the main passage and one entrance to the outside. In addition, several active fumaroles or fumarole fields exist in this hall, which explains the large size of the room. Here both the highest maximum and nearly the lowest minimum of all measurement locations were recorded. One of the strongest fumaroles found is located a few meters below the temperature sensor.

The Lakes site is immediately adjacent to Adélie Lake (Fig. 6a), approximately one meter above the water level; this area is also unaffected by fumaroles. Results here correspond predominantly with the neighboring Main Passage 2 site, but exhibit stronger overall cold air intrusions from the Subway Entrance, which is also underscored by the low annual mean temperature of 1.2 °C.

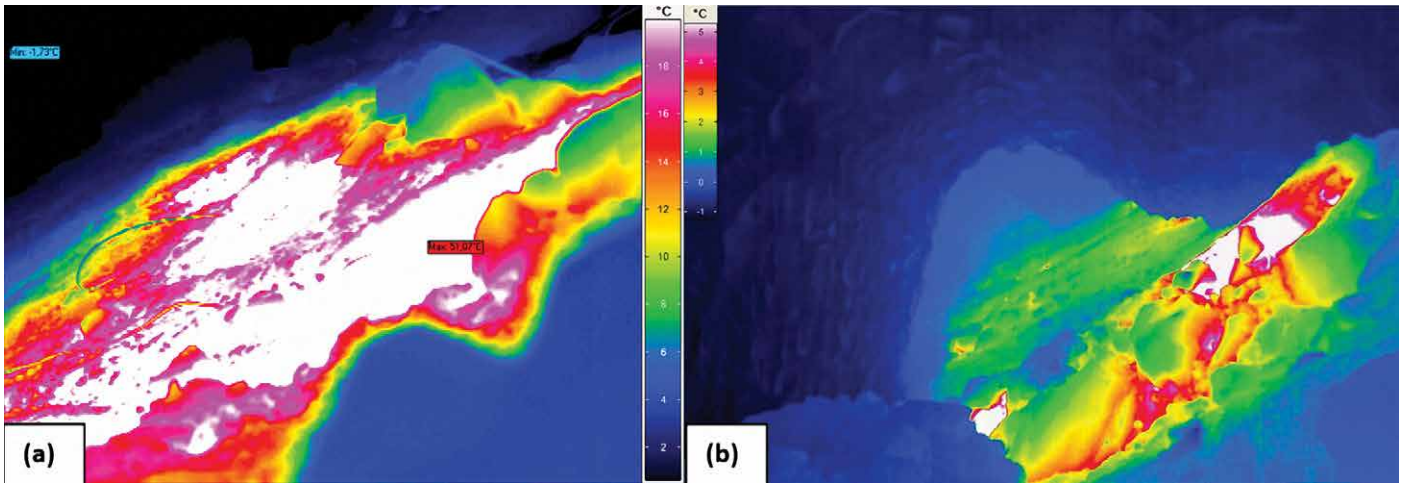

Figure 7. East Crater Cave thermographic investigations, observations, and fumarole information. (a) Representative thermographic image from video recording showing a 51 °C hot spot (labelled within image) on the crater floor inside East Crater Cave, located near the High Noon entrance. Temperature minima in the image is 1.7 °C. (b) Representative thermographic image from video recording of the laterally oriented main passage in East Crater Cave. Fumarolic heat and hot spots can be observed on the crater floor from 1 °C to 5 °C. The image shows two areas of heated ground separated by a colder area. The areas of heated ground correspond to wider dome shaped rooms that are interconnected by slightly narrower passages.

DISCUSSION

When glacial ice superimposes an active volcanic edifice, localized heat transfer causes ice melt. The result is glaciovolcanic caves (Sobolewski, et al., 2022a). *A priori*, the scope, scale, and shape of these glaciovolcanic caves very much depends upon the mode and magnitude of heat transfer, and the rate of accumulation and movement of the glacial ice. The persistence of a glaciovolcanic cave is therefore dependent upon continued volcanic heat flux and a favorable climate for glacial ice accumulation. When heat flux ends and fumaroles cease, plastic deformation of glacial

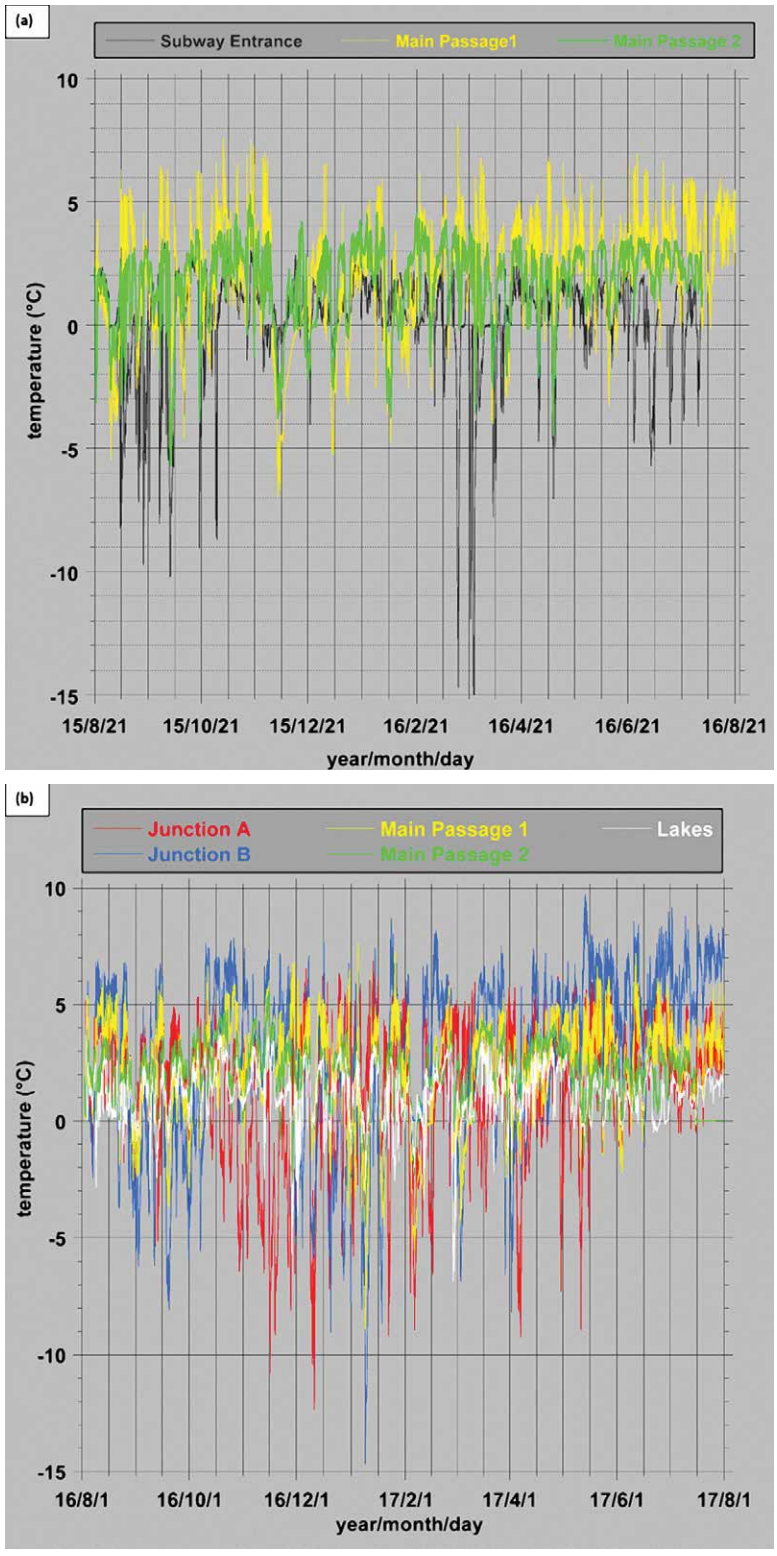

Figure 8. (a) Air temperature (°C) from the three cave passages measured from August 2015 to August 2016. (b) Air temperature (°C) from the five cave passages measured from August 2016 to August 2017.

ice will squeeze these caves closed. In contrast, when climate warms and snowfall ceases, melt will daylight and eventually eliminate these caves, such as those on the Paradise Ice Field of Mount Rainer (Anderson et al., 1994). In short, glaciovolcanic caves are ephemeral phenomena.

The Cascade Volcanic Arc in the Pacific Northwest of the United States is a valuable laboratory for investigations of glaciovolcanic caves. At Mount Hood, the caves in the Sandy Glacier are shrinking as the glacier retreats (Pflitsch et al., 2017). At Mount Saint Helens, the caves are expanding as Crater Glacier grows (Sobolewski et al., 2022b). In contrast, exploration at the summit of Mount Rainier reveals a system of glaciovolcanic caves that persist for at least a half-century. We suspect that the high elevation, bowl-like summit craters and persistent fumaroles have culminated in a stable setting for these glaciovolcanic caves. It is not evident that these caves at the summit of Mount Rainier are in equilibrium, however.

Glaciovolcanic Caves at the Mount Rainier Summit are in Dynamic Equilibrium

Direct measurements of passage cross section in the two measured areas of the circumferential passage, East of Lake Adélie and at the Coliseum, show no detectable change in passage dimensions from 2016 to 2017 (Table 5) given the expected survey error. Furthermore, the debris ridges along the bottom of the circumferential passage reported in Kiver and Steele, (1975) were present in 2015, 2016, and 2017 and of similar distance to the cave walls, conveying consistency in main passage size and position. (Fig. 9a). More generally, the scale and position of the circumferential passage shows consistency across all included maps. The one exception are the sections west of Lake Adélie where the circumferential passage alternates from shallower to deeper parts of the crater over the past half century in an area devoid of fumaroles during the 2015−2017 survey (Fig. 5).

Ice movement in the crater has not been accurately measured. Tephra layers and strain indicators in the East Crater Cave suggest a west to east horizontal direction of movement from Columbia Crest. Vertical rates of ice motion were estimated by Kiver and Steele (1975) to be 1.66 m y^{-1} to 2.65 m y^{-1} and 2.05 m y^{-1} to 3.48 m y^{-1} in the East Crater and West Crater Caves, respectively, using similar methodology but over a maximum 11 days' timeframe. Our single estimate of 8.4 m y^{-1}, while noteworthy, is not conclusive of an increase in ice motion since the 1970s despite higher rates of glacial retreat on the edifice flanks (Anderson and Shean, 2022).

Despite this ice motion, most of the circumferential passage has remained much the same over 47 years (Fig. 5); fumaroles and heated rock persisted at the same locations for decades and air flow maintains the connections between

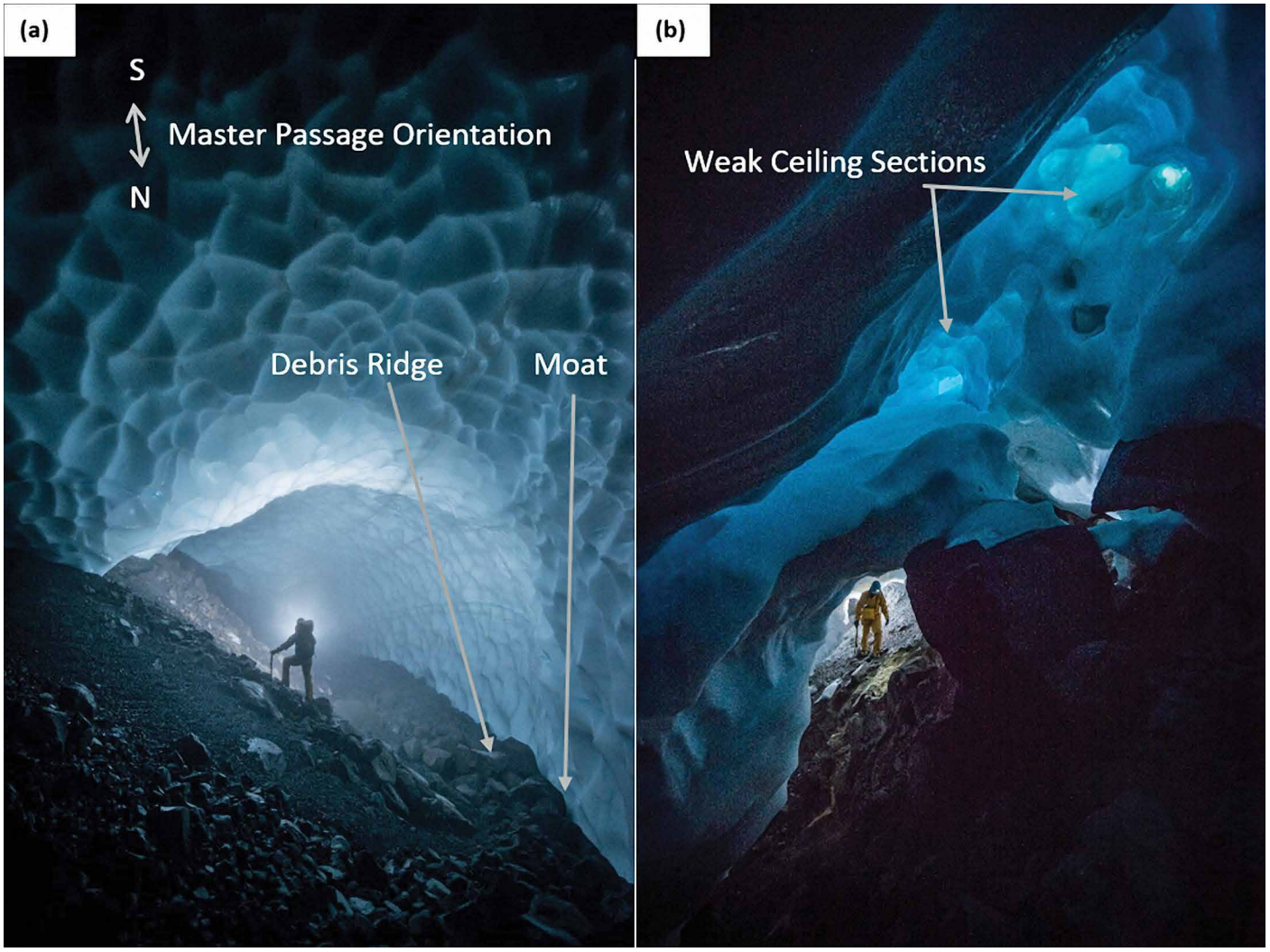

Figure 9. (a) Typical passage in the East Crater cave master circumferential passage. Debris build up against the inner side of the ring (right side) passage buttresses a small moat, as observed in 1973 (Kiver and Steele, 1975). (b) Upper-level cave passages display numerous skylights, weak spots in ceilings, and occasional debris collapse.

these areas of heat flux. As the glacial ice moves, it deforms around the open void and squeezes shut downslope of the zone of heat flux. Thus, most of the circumferential passage has achieved a dynamic equilibrium where the exact position and shape may vary from year to year below a threshold value as governed by sensitivities to external and internal forcing (Florea et al., 2021). These sections of cave contour the curvilinear strike of the crater (Appendix 1), are sub-horizontal (Table 4), and are more or less conserved in the decadal timespan of this synthesis (Fig. 5; Table 3).

Of interest is the absence of cave passage on the west side of East Crater prior to the 2015−2017 expeditions that added 598 m of mapped passage in that area (Fig. 4a). Also curious is the position of the circumferential passage connecting this western extension to Lake Adélie and points east (Figs. 4a and 5). In the case of the former, the increase may potentially source to previous inaccessibility of these passages or to increased fumarole activity near Columbia Crest. Smaller average passage diameters (4.8 m) than elsewhere in East Crater Cave (6.6 m) may suggest a younger state of development for the extension (Fig. 10a). In the case of the later, this connecting passage is dramatically different in all four surveys (Fig. 5), perhaps increased ice movement in this section sweeps passages at the crater rim away from their originating fumaroles where they are maintained only by significant advection until they squeeze shut and the process is repeated. These sections of cave, as well as most other passages steeply rising to or following the crater rim (Fig. 4; Appendix 1) are dendritic feeders or distributaries of fumarole advection and dynamically change throughout the timeline of this synthesis (Table 4).

Microclimates Influence Passage Equilibrium

The synthesis of a year-long dataset of cave and fumarole temperature, air pressure, and water level in Lake Adélie conducted by Florea et al. (2021) was a detailed look into high-frequency (15-minute) changes in the microclimate en-

Figure 10. (a) Typical passage in the East Crater cave, NW extension, passages trending upwards towards the crater rim display low, wide forms. (b) Hazmat Entrance, East Crater Cave, showing a passage collapse.

vironment of a small portion of the Mount Rainier glaciovolcanic caves. That study investigated the seasonality of these caves; as the winter snowfall season seals entrances, advection diminishes, and convection dominates until melt-out reopens the entrances and resets the system. That study, without direct evidence, inferred short term changes in the size of the circumferential passage linked to melt rate. It also noted the changing size and position of entrances through time. Maps and data from this study document those changes over a punctuated decadal timespan. Inter-annual temperature monitoring presented herein span the cave floorplan, and thus are more representative of system-wide variation through time.

At first glance (Table 4), the summary statistics reveal that conserved sections of cave that are in dynamic equilibrium (three dataloggers) have warmer average temperatures with smaller variation about the mean (T_{ave} = 1.8 °C, σ = 3.2 C°; T_{min} = −7.4 °C, and T_{max} = 6.4 °C). These passage segments are larger (D_{ave} = 7.4 m) and concentrate in the circumferential passage and the bigger persistent Subway entrance and Bird Room. In contrast, sections of cave that are transient (five dataloggers) have cooler average temperatures with greater variation about the mean (T_{ave} = 1.4 °C, σ = 8.0 C°; T_{min} = −12.3 °C, and T_{max} = 7.8 °C). These passage segments are smaller (D_{ave} = 3.8 m) and concentrate along the crater rim, including most entrances and the passages that connect to the deeper cave, including the circumferential passage west of Lake Adélie. In these sections of cave where solar insolation can be strong, oscillating ventilation of fumarole steam and incursions of cold air are interrupted by winter snowfall occlusion.

A deeper dive at a few datalogger sites provides additional context. The Subway Entrance (persistent across the suite of survey maps) experiences regular intrusions of cold outside air in the spring and autumn months and records the lowest minimum, maximum, and average temperatures among the sites (T_{ave} = 0.12 °C, σ = 4.6 C°; T_{min} = −15.5 °C, and T_{max} = 3.3 °C). These same intrusions are missing in the winter when they would be most expected. Instead, the winter data are relatively stable near 0 °C and support an entrance closure by snowpack described in Florea et al. (2021) using dataloggers at Lake Adélie.

In the circumferential passage, and below the Subway Entrance, air temperature data greatly stabilizes near Lake Adélie (T_{ave} = 1.2 °C, σ = 1.4 C°; T_{min} = −6.9 °C, and T_{max} = 5.4 °C). The cool but predominantly balanced temperature conditions are underlined by the low variance of 1.4 °C. Air warms counterclockwise along an eastward path of advection toward the Coliseum, fumarole areas, and the Main Passage 2 area below the Guide Rocks Entrance (T_{ave} = 2.3 °C, σ = 4.7 C°; T_{min} = −8.9 °C, and T_{max} = 7.7 °C) where pulses of cold air occasionally descend. Main Passage 2 showed the highest temperature peaks of the conserved passages. There, influence by air heated by fumarole outgassing from the neighboring hall is convectively led into the upper areas of the space and exhausted via the elevated connecting passage. The comparatively high variance of 4.8 C° within this hall is likely due to cold air infiltration from the Guide Rocks entrance.

Results rarely showed lower temperature minima than Main Passage 1, falling well below 5 °C only once. The maxima are lower than at Main Passage 1 almost year round but still often significantly higher than the values of the Subway Entrance.

Similarly, temperatures near the Pinnacles Entrance (T_{ave} = 1.4 °C, σ = 8.2 C°; T_{min} = −12.4 °C, and T_{max} = 6.8 °C) warm and stabilize along a clockwise path of advection past the fumarole field below the Yeti Entrance (T_{av} = 2.8 °C, σ = 13.7 C°; T_{min} = −14.7 °C, and T_{max} = 9.6 °C) toward Hobo Point (T_{ave} = 1.7 °C, σ = 3.8 C°; T_{min} = −9.5 °C, and T_{max} = 6.4 °C) and the area below the Aircrash Entrance (T_{ave} = 1.9 °C, σ = 1.8 C°; T_{min} = −4.5 °C, and T_{max} = 5.6 °C). The section of circumferential passage centered on the Coliseum, where advection paths converge and heated areas concentrate (Fig. 5), has remained exceptionally consistent for a half century.

Morphodynamic Model for Glaciovolcanic Caves

Glaciovolcanic cave morphology is minimally classified compared to the detail applied to caves formed in soluble rocks (e.g., Ford and Williams, 2007). We used this and similar studies at Mount Saint Helens (Sobolewski et al., 2022b) and Mount Hood (Pflitsch et al. 2017) to arrive at similar detailed characterizations. A key difference is the rate of change in these settings, which matches the pace of change in some coastal environments where the morphology is highly dynamic across decadal and shorter timescales. We borrow and apply the term morphodynamic from that literature to highlight the connection between the pace of change and the resultant morphology (Wright and Thom, 1977). This study is one window into that connection.

The balance between heat flux and climate guides the pace of development and the longevity of glaciovolcanic caves. When those two factors are balanced, passages that originate around and connect fumarole areas will persist, and the pace of ice ablation by melt matches the rate of ice replacement by glacial movement. In contrast, when those two factors are not balanced, melt will daylight the caves or ice movement will squeeze the passages closed. In reality, both processes occur in all glaciovolcanic settings; nowhere do these factors balance at the timescale of glaciovolcanic cave evolution, even on Mount Rainier where the summit caves have persisted for at least a half century.

In this study, and comparing our data to prior expeditions, we are able to divide the East Crater Cave on Mount Rainier into two primary categories, passages that are transient and those that are conserved in a dynamic equilibrium. Most of the circumferential passage has remained remarkably consistent, maintaining a similar position, scale, and morphology over a 47-year timespan. Consistency in reported main passage length, depth, and

Figure 11. Entrance zones of cave passages in East Crater Cave without direct fumarolic influence. (a) Snow and debris on floor extends into the cave. (b) Walking and crawling passages are shown while ice walls typically connect directly to the floor at the rock-ice margin with no airspace.

dimensions (Table 3), along with visual observation of debris ridges (Kiver and Steele, 1975) demonstrate the similarity. Our detailed cross-section measurements from one year to the next could not resolve any change in size and point to consistent passage scale. As west-to-east advection in this passage connects dome shaped rooms above heated rock and active fumaroles, temperatures warm (T_{ave} = 1.2–1.4 °C); and stabilize (σ = 1.4–4.7 C°) and passage equilibrium increases.

Passages that are transient tend to be smaller in diameter (3.8 m compared to 7.4 m) and are subject to higher temperature fluctuation (σ = 8.0 C° compared to 3.2 C°), and concentrate along the crater rim, but include some passages that connect the rim by advection to the deeper circumferential passage (Fig. 11a and b). Fumaroles maintain passage development here too (Fig. 12). Seasonal weather extremes, however, are not buffered by the heat capacity of the ice. In the summer, meltout can, and does, occur from fumarole heat and solar insolation (Fig. 9b), while mechanical collapse can occur as well, restricting airflow and potentially blocking entrances (Fig. 10b). In the winter, some entrances are sealed shut by accumulated snowfall and bitter cold. Disparate numbers of surveyed entrances across the study timeframe confirm the transience (Table 3). The compaction of firn to ice as snowfall maintains the glacial plug means that some passages are swept away from their heat source. The results point towards a situation where the deeper circumferential passages within the Mount Rainier system are not as influenced by seasonal weather and maintain a dynamic equilibrium (Florea et al., 2021). The upper ring of fumaroles, while they may maintain open passages, are too influenced by external factors to remain conserved over time. Fig. 13 visualizes these two primary categories and their existence within the dynamic equilibrium.

Broader Implications

The potential for Cascade volcanoes, such as Mount Rainier, to impact large population centers drives the need for longitudinal studies. Changes within a volcanic system causing alteration of glaciovolcanic void morphology can make them a volcano monitoring and hazard indicator (Curtis and Kyle, 2017). Longitudinal-morphology studies may identify conserved and transient glaciovolcanic cave passages as normal conditions on an edifice. Unlike nearby glaciovolcanic caves on Mount Saint Helens that are expanding (Sobolewski et al., 2022b) and Mount Hood that are retreating (Pflitsch et al., 2017) and not in dynamic equilibrium, any sudden and dramatic changes in glaciovolcanic cave morphology on

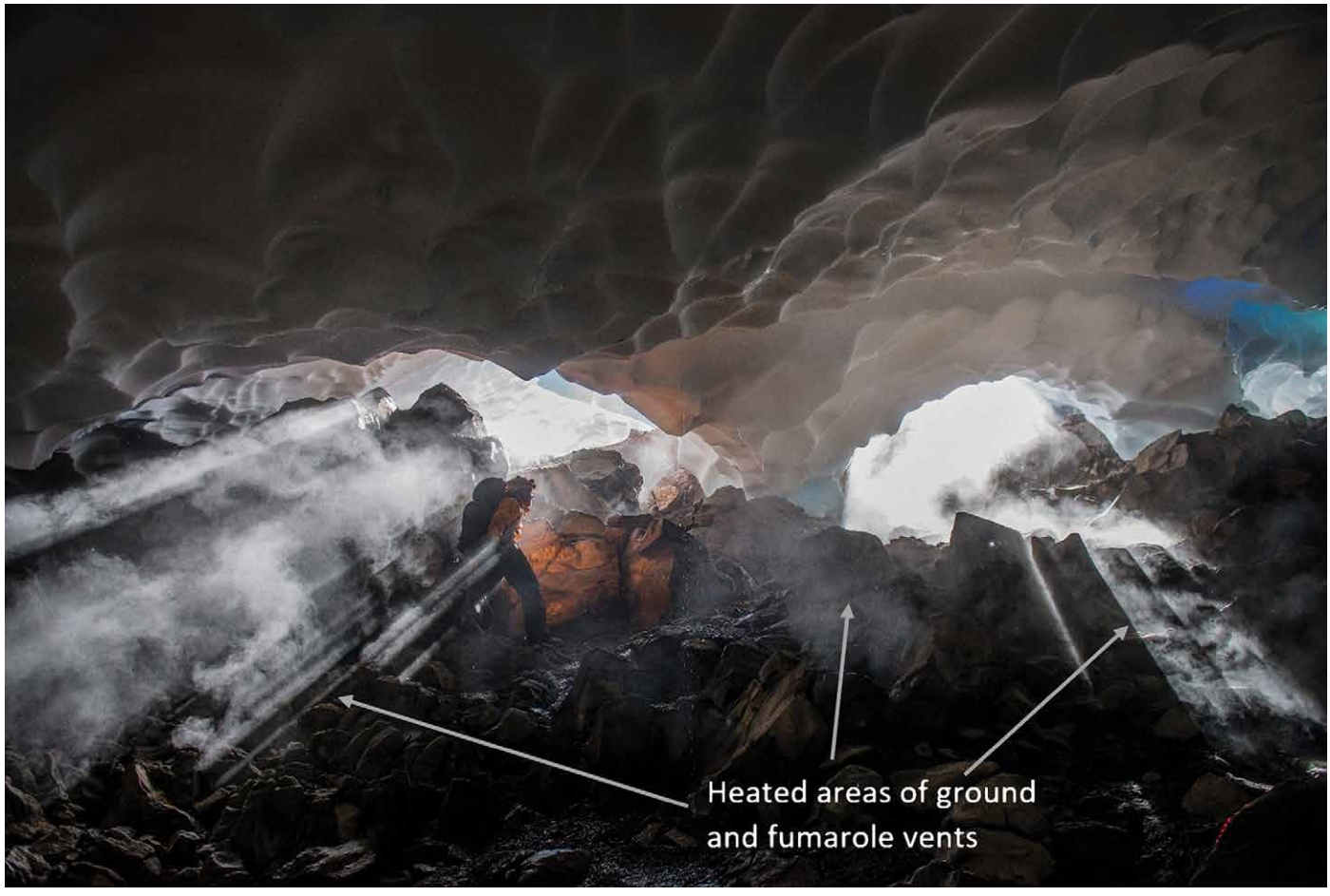

Figure 12. Entrance zones of cave passages in East Crater Cave with direct fumarolic influence (Murphy's Law entrances).

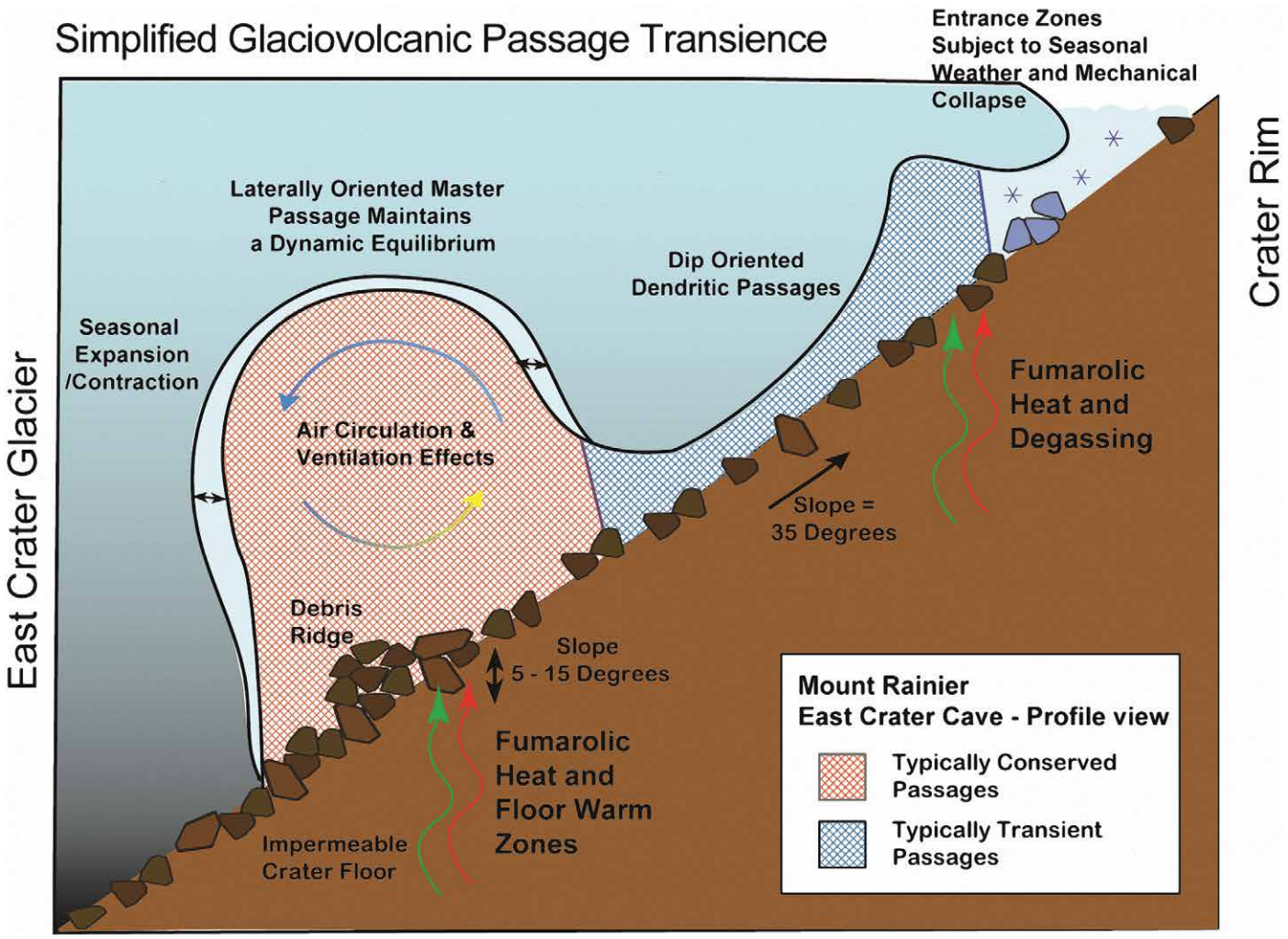

Figure 13. Cross-section diagram of the passages within the Mount Rainier system showing typical lateral and dip-oriented passages. Master circumferential passage with dynamic equilibrium is conserved while transient passages radiate from the master passage towards ephemeral entrances and entrance zones.

the Mount Rainier summit or similar edifices are a heightened cause for concern and worthy of further investigations. Accurate detection of changes to volcanic activity by other methods (e.g., aerial and satellite remote sensing, deformation monitoring, or increased seismicity) may not always capture early changes to heat flux on a glaciated edifice where the ice may absorb considerable heat output; the direct sublimation 1 g of ice at 0 °C to water vapor or the phase change of that ice to fumarole steam at 100 °C requires heat inputs of 2838 J or 6750 J, respectively. Put another way, existing conserved glaciovolcanic cave passages and other subglacial voids may enlarge substantially, and/or transient passages may multiply. These potential observations can be made before other changes on the edifice are measurable or before externally visible changes occur due to increased heat input.

Limitations of this study include the reliance on historical data with disparate collection and survey methodologies. To accurately demonstrate the changes observed in passages with rapidly evolving position and morphology, and to compute ablation rates in relatively stable passages (Florea et al., 2021) will take sequential mapping over several years, using techniques such as LiDAR or Simultaneous localization and mapping (SLAM), to produce timelapse 3D maps. Collecting a full inventory of temperature, relative humidity, and airflow data along with ice ablation and calculated heat flux will assist to explain formation mechanisms and verify new analytical and numerical models (e.g., Unnsteinsson, 2022) Such evolution in mapping and understanding glaciovolcanic environments has further implications as we look beyond terrestrial examples to thermal influences on ice-covered ocean worlds. The microclimates and morphologies of glaciovolcanic caves can leverage hypotheses of similar environments elsewhere in the solar system and provide insight into perennially cold, dark, oligotrophic ecosystems like frozen Martian cave systems hypothesized to be the most accessible location of current life or intact biomarkers. (Sobolewski, et al., 2022a; Curtis, 2020; Davis et al., 2020; Tebo et al, 2015). Understanding the factors influencing long term longevity of void spaces in ice can play a role in these investigations.

CONCLUSIONS

The East Crater Cave at Mount Rainier, at 3593 m in length and 144 m in depth is a significant example of a glaciovolcanic cave that provides insight into the dynamics of this subset of speleology. Comparative measurements of statistical information and historical surveys of the Mount Rainier glaciovolcanic caves over decadal timescales, from 1970−2017, provided insight into glaciovolcanic cave passage morphodynamics. The caves exhibit distinct morphology patterns and have expanded in the 47 years since the first reported survey results.

Comparisons revealed persistent circumferential master passages with characteristically similar low gradient sub-horizontal lateral orientations following the curvilinear crater contour. Two persistent entrances and the cave low point were also characterized. These passages are considered conserved given positional and geometric similarity over time but with vertical ice advection around a consistent passage form. Persistent passages displayed stable temperatures, or where temperatures varied, were influenced by adjacent fumarole activity. Persistent fumaroles and heated floors assist in maintaining the master passage in position and form.

Transient passages were revealed with smaller average diameters and larger temperature variances. A previously undocumented extension of 598 m on the west side of the East Crater had smaller diameter passages. Transient passages were the most thermally unstable and were potentially influenced by snowpack accumulation and entrance collapses. Entrance zones exhibit seasonal and long-term transient morphology, whereby snowpack and collapse combined with persistent fumarolic output and pressure drive competitive development of new outlet passages originating radially from the conserved source passages. Morphodynamic factors influencing these glaciovolcanic cave passage types include non-linear ice dynamics and point source and area heat fluxes and require additional research to understand.

ACKNOWLEDGEMENTS

Financial and equipment support from National Geographic Expeditions Council, the Mazamas Research Grant, the Mountain Rescue Association, Petzl, REI, Alberta Speleological Society and National Speleological Society. Aaron Messinger and Special Projects Operations, supplier of SCBA equipment. Eugene Kiver, Bill Lokey, and Aaron Curtis for helpful advice and support. Additional cave surveyors 2015−2017, Tabbatha Cavendish, Kathleen Graham, John Punches, Nick Vieira, and Barb Williams. Tom Wood, Tom Gall, and Woody Peeples for their safety and medical support. Cracker Jack First Response Specialists facilitated logistics for the 2015 field portion. John Meyers and Dave Clarke coordinated porter teams. The over 100 personnel who facilitated the studies by portering scientific and expedition equipment to the summit and back, supported by Corvallis Mountain Rescue (OR), Deschutes Mountain Rescue (OR), Everett Mountain Rescue (WA), Hood River Crag Rats (OR), Olympic Mountain Rescue (WA), Portland Mountain Rescue (OR), Volcano Rescue Team (WA), Douglas County Sheriff's Mountain Rescue Unit (OR). Research and collecting permit from the United States Department of the Interior National Park Service–Mount Rainier.

REFEENCES

Anon., 1972, Climber reports change, Mount Rainier steam tunnels heating up, *in* Halliday, W.R., ed., The Cascade Caver, v. 12, no. 8, p. A-13.

Anderson, S.W., and Shean, D., 2022, Spatial and temporal controls on proglacial erosion rates: A comparison of four basins on Mount Rainier, 1960 to 2017: Earth Surface Processes and Landforms, v. 47, no. 2, p.596−617. https://doi.org/10.1002/esp.5274

Anderson, C.H., Vining, M.R., and Nichols, C.M., 1994, Evolution of the Paradise/Stevens Glacier Ice Caves: Bulletin of the National Speleological Society, v. 56, no. 2, p. 70–81.

Anderson, C. H., Behrens. C. J., Floyd, G. A., and Vining, M. R., 1998, Crater Firn Caves of Mount St. Helens, Washington: Journal of Cave and Karst Studies, v. 60, no. 1, p. 44–50.

Benn, D., Gulley, J., Luckman, A., Adamek, A., and Glowacki, P. S., 2009, Englacial drainage systems formed by hydrologically driven crevasse propagation: Journal of Glaciology, v. 55, no. 191, p. 513−523.

Capra, L., 2008, Abrupt climatic changes as triggering mechanisms of massive volcanic collapses: Journal of Volcanology and Geothermal Research, v. 155, p. 329–333. https://doi.org/10.1016/j.jvolgeores.2006.04.009

Cartaya, E., 2016, MRA Coalition Supports International Mount Rainier Cave Study: Meridian, San Diego, CA. p. 5−10.

Crandell, D. R., 1971, Postglacial lahars from Mount Rainier volcano, Washington: U.S. Geological Survey Professional Paper 677, Washington, DC: United States Government Printing Office, p. 75.

Curtis, A., 2020, Comparison of Earth's fumarolic ice caves, with implications for icy voids on other worlds [abs.]: 3rd International Planetary Caves Conference, San Antonio, Texas. 1 p.

Curtis, A., 2016, Dynamics and global relevance of fumarolic ice caves on Erebus Volcano, Antarctica [Ph.D. thesis]: Socorro, New Mexico Institute of Mining and Technology, https://aaroncurt.is/paper/curtis2016-phd_diss.pdf (Accessed 28 August, 2020).

Curtis, A., 2010, Erebus Cave and Fumarole Database. Available from: http://erebuscaves.nMountedu/ (Accessed April 12, 2021).

Curtis, A. and Kyle, P., 2017, Methods for mapping and monitoring global glaciovolcanism: Journal of Volcanology and Geothermal Research, v. 333–334, p. 134–144. https://doi.org/10.1016/j.jvolgeores.2017.01.017

Curtis, A. and Kyle, P., 2011, Geothermal point sources identified in a fumarolic ice cave on Erebus volcano, Antarctica using fiber optic distributed temperature sensing: Geophysical Research Letters, v. 38, no. 16, p. L16802. doi: 10.1029/2011GL048272

Davis, R., Anitori, R., Stenner, C., Smith, J., and Cartaya, E., 2020, Fumarolic glacial and firn ice caves on Mount St. Helens may provide insight into Martian subsurface microbial communities [abs.]: Analog Field Sites Mini Symposium, Houston, Texas. The Lunar and Planetary Institute, Open University Astrobiology, and NASA Johnson Space Center.

Edwards, B., Kochtitzky, W., Battersby, S., 2020, Global mapping of future glaciovolcanism: Global and Planetary Change, v. 195, p. 103356. https://doi.org/10.1016/j.gloplacha.2020.103356

Ewert, J.W., Diefenbach, A.K., and Ramsey, D.W., 2018, 2018 update to the U.S. Geological Survey national volcanic threat assessment: U.S. Geological Survey Scientific Investigations Report 2018–5140, 40 p. https://doi.org/10.3133/sir20185140

Finn, C. A., Sisson, T. W., and Deszcz-Pan, M., 2001, Aerogeophysical measurements of collapse-prone hydrothermally altered zones at Mount Rainier volcano: Nature, v. 409, p. 600–603. https://doi.org/10.1038/35054533

Fish, L., 2020, Compass Cave Survey Software for Windows [Computer software]. https://fountainware.com/compass/index.htm (Accessed August 28, 2020).

Florea, L., Pflitsch, A., Cartaya, E., and Stenner, C., 2021, Microclimates in fumarole ice caves on volcanic edifices—Mount Rainier, Washington, USA: Journal of Geophysical Research Atmospheres. v. 126, no. 4, p. 1−15. https://doi.org/10.1029/2020JD033565

Ford, D., and Williams, P. D., 2007, Karst Hydrogeology and Geomorphology: Chichester, West Sussex, England, John Wiley & Sons.

Frank, D., 1995, Surficial extent and conceptual model of hydrothermal system at Mount Rainier, Washington: Journal of Volcanology and Geothermal Research, v. 65, no. 1, p. 51−80. https://doi.org/10.1016/0377-0273(94)00081-Q

Gambino, S., Armienti, P., Cannata, A., Del Carlo, P., Giudice, G., Giuffrida, G., and Pompilio, M., 2021, Mount Melbourne and Mount Rittmann: Geological Society, London, Memoirs, v. 55, no.1, p. 741−758.

Giggenbach, W. F., 1976, Geothermal ice caves on Mt Erebus, Ross Island, Antarctica: New Zealand Journal of Geology and Geophysics, v. 19, no. 3, p. 365–372. https://doi.org/10.1080/00288306.1976.10423566

Gulley, J.D., and Fountain, A.G., 2019, Glacier Caves, *in* White, W.B., Culver, D.C., Pipan, T., eds., Encyclopedia of Caves, 3rd edition: Cambridge, Mass., Academic Press. https://doi.org/10.1016/B978-0-12-814124-3.00056-X.

Halliday, W.R., 2007. Pseudokarst in the 21st century: Journal of Cave and Karst Studies, v. 69, no. 1, p. 103−113.

Häuselmann, P., ed., 2012, UIS Mapping Grades. Version 2. Survey and Mapping Working Group, UIS Informatics Commission http://www.uisic.uis-speleo.org/UISmappingGrades.pdf (Accessed June 14, 2020).

Heeb B., 2009, An all-in-one electronic cave surveying device: Cave Radio and Electronics Group Journal, v. 72, p. 8-10.

Heeb, B., n.d., Paperless Cave Surveying. https://paperless.bheeb.ch/ (Accessed June 14, 2020).

Holler, C., 2019. Chapter 101 – Pseudokarst. *in* White, W.B., Culver, D.C., Pipan, T, eds., Encyclopedia of Caves, 3rd edition: Cambridge, Mass., Academic Press. https://doi.org/10.1016/B978-0-12-814124-3.00101-1

Hoblitt, R.P., Walder, J.S., Driedger, C.L., Scott, K.M., Pringle, P.T., and Vallance, J.W., 1998, Volcano hazards from Mount Rainier, Washington, revised 1998: U.S Geological Survey Open-File Report p. 98–428. https://pubs.usgs.gov/of/1998/0428/.

Hoffman, R., Woodward, A., Haggerty, P., Jenkins, K. J., Griffin, P. C., Adams, M.J., Hagar, J., Cummings, T., Duriscoe, D., Kopper, K., Riedel, J.L., Marin, L., Mauger, G., Bumbaco, K., and Littell, J.S., 2014, Mount Rainier National Park—Natural resource condition assessment: National Park Service, Natural Resource Report NPS/MORA/NRR-2014/894, 380 p.

Kiver, E.P., and Mumma, M.D., 1971, Summit firn caves, Mount Rainier, Washington. Science, v. 173. p. 320−322. https://doi.org/10.1126/science.173.3994.320

Kiver, E.P., and Steele, W.K., 1975, Firn caves in the volcanic craters of Mount Rainier: The National Speleological Society Bulletin. v. 37, no. 3. p. 45−55.

Korosec, M.A., 1989, Geothermal resource evaluation of Mount Rainier. Lacey, WA: U.S. Department of Interior, Bureau of Land Management, p. 61.

Le Guern, F., Ponzevera, E., Lokey, W, and Schroedel, R.D., 2000, Mount Rainier summit caves volcanic activity: Washington Geology, v. 28, no. 1/2, p. 25.

Liuzzo, M., Giudice, G., Giuffrida, A.C., 2018, Investigation of Ice-Caves on Melbourne and Rittman volcanoes, Antarctica [presentation]. European Geosciences Union General Assembly 2018, Vienna, Austria, 8−13 Apr. https://www.icevolc-project.com/presentations (Accessed April 8, 2021).

Lokey, W.M., 1973, Crater studies at a sleeping volcano: Explorers Journal., v. 51, p. 167−170.

Lokey, W.M., Mack, R., Miller, M.M., Prather, B.W. and Kiver, E.P., 1972, Project Crater: Mount Rainier glacio-volcanological research, 1970−72. [abs.]: Arctic and Mountain Environments Symposium, Michigan State University.

National Research Council, 1994, Mount Rainier: Active Cascade Volcano. Washington, D.C., The National Academies Press. https://doi.org/10.17226/4546

Nylen, T. H., 2004, Spatial and temporal variations of glaciers (1913−1994) on Mount Rainier and the relation with climate [Master's thesis]: Portland, OR, Portland State University.

Pflitsch, A., Cartaya, E., McGregor, B., Holmgren, D., and Steinhöfel, B., 2017, Climatologic studies inside Sandy Glacier at Mount Hood Volcano in Oregon, USA: Journal of Cave and Karst Studies, v. 79, no. 3, p. 189-206. http://dx.doi.org/10.4311/2015IC0135

Roberti, G., 2018, Mount Meager, a glaciated volcano in a changing cryosphere: hazards and risk challenges. [PhD. Thesis]: Earth Sciences, Université Clermont Auvergne. https://www.researchgate.net/publication/330980980_Mount_Meager_a_glaciated_volcano_in_a_changing_cryosphere_hazards_and_risk_challenges (Accessed August 18, 2020).

Sauro, F., Pozzobon, R., Massironi, M., De Berardinis, P., Santagata, T., De Waele, J., 2020, Lava tubes on Earth, Moon and Mars: A review on their size and morphology revealed by comparative planetology: Earth-Science Reviews, v. 209, p. 103288. https://doi.org/10.1016/j.earscirev.2020.103288

Scott, K.M., Vallance, J.W., and Pringle, P.T., 1995, Sedimentology, behavior, and hazards of debris flows at Mount Rainier: U.S. Geological Survey Professional Paper 1547, Washington, D.C.: U.S. Geological Survey, 56, p.

Sisson, T.W., Robinson, J.E., and Swinney, D.D., 2011, Whole-edifice ice volume change A.D. 1970 to 2007/2008 at Mount Rainier, Washington, based on LiDAR surveying: Geology, v. 39, p. 639–642. https://doi.org/10.1130/G31902.1

Sisson, T.W. and Vallance, J.W., 2009. Frequent eruptions of Mount Rainier over the last ~2,600 years: Bulletin of Volcanology, v. 71, no. 6, p. 595−618. https://doi.org/10.1007/s00445-008-0245-7

Sobolewski, L., Hansteen, T., Zorn, E., Stenner, C., Florea, L., Burgess, S., Ionescu, A., Cartaya, E., and Pflitsch, A., 2023, The evolving volcano-ice interactions of Crater Glacier, Mount St. Helens, Washington (USA): Bulletin of Volcanology, v. 85, no. 22. https://doi.org/10.1007/s00445-023-01632-5

Sobolewski, L., Stenner, C., Williams-Jones, G., Anitori, R., Davis, R., 2022a, Implications of the study of subglacial volcanism and glaciovolcanic cave systems: Bulletin of Volcanology, v. 84, no. 21. https://doi.org/10.1007/s00445-022-01525-z

Sobolewski, L., Stenner, C., Hüser, C., Berghaus, T., Cartaya, E., and Pflitsch, A., 2022b, Ongoing genesis of a novel glaciovolcanic cave system in the crater of Mount St. Helens, Washington, USA: Journal of Cave and Karst Studies, v. 84, no. 2, p. 51−65. https://doi.org/10.4311/2021ES0113

Stenner, C., Pflitsch, A., Florea, L., Graham, K., Cartaya, E., 2022, Development and persistence of hazardous atmospheres within a glaciovolcanic cave system—Mount Rainier, Washington, USA: Journal of Cave and Karst Studies, v. 84, no. 2, p. 66−82. https://doi.org/10.4311/2021EX0102

Stenner, C., Sobolewski, L., Pflitsch, A. and Cartaya, E., 2020, Morphology of a new system of glaciovolcanic caves—Mount St. Helens, Washington, USA, [C038-0001], American Geophysical Union, 2020 Fall meeting. https://www.essoar.org/doi/10.1002/essoar.10505755.1

Stevens, H., 1876, The ascent of Takhoma: Atlantic Monthly, Nov., p. 511−530.

Tebo, B. M., Davis, R. E., Anitori, R. P., Connell, L. B., Schiffman, P., and Staudigel, H., 2015, Microbial communities in dark oligotrophic volcanic ice cave ecosystems of Mount Erebus, Antarctica: Frontiers in Microbiology, v. 6, no. 179. https://doi.org/10.3389/fmicb.2015.00179

Tuffen, H., 2010, How will melting of ice affect volcanic hazards in the twenty-first century?, Philosophical Transactions of the Royal Society A, v. 368, p. 2535–2558. https://doi.org/10.1098/rsta.2010.0063

Unnsteinsson, T., 2022, Modelling glaciovolcanic caves and chimneys [M.Sc. thesis]: Burnaby, Simon Fraser University. https://www.sfu.ca/content/dam/sfu/volcanology/pdfs/Theses/Unnsteinsson_MSc'22.pdf (Accessed October 10, 2022).

Vallance J.W., Scott K.M., 1997, The Osceola mudflow from Mount Rainier: Sedimentology and hazards implications of a huge clay-rich debris flow: Geological Society of America Bulletin, v. 109, p. 143–163. https://www.morageology.com/pubs/59.pdf (Accessed July 5, 2023).

Wilkins, J., 1970, 2 Climbers Thread Needle, Penetrate Rainier Tunnels: Tacoma News Tribune, June 21, 1970: Tacoma, Washington USA.

Whittaker, J., 1957, Jim Whittaker letter to Dee Molenaar regarding exploration of Mount Rainier steam cave, January 15, 1957 https://www.omnia.ie/index.php?navigation_function=2andnavigation_item=04d5d055dee795a53479ec24bacf2b63andrepid=2 (Accessed May 4, 2021).

Wright, L.D., and Thom, B.G., 1977, Coastal depositional landforms: a morphodynamic approach: Progress in Physical Geography, v. 1, no. 3, p. 412−459.

Zimbelman, D.R., Rye, R.O., and Landis, G.P., 2000, Fumaroles in ice caves on the summit of Mount Rainier—preliminary stable isotope, gas, and geochemical studies: Journal of Volcanology and Geothermal Research, v. 97, p. 457–473, https://doi.org/10.1016/S0377-0273(99)00180-8